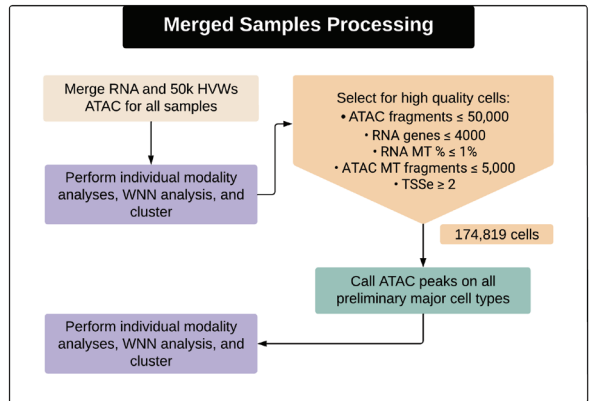
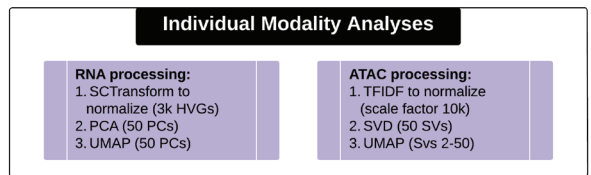
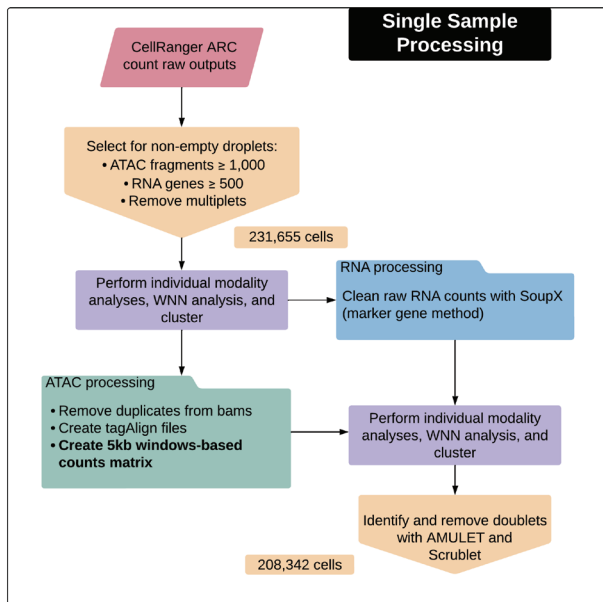
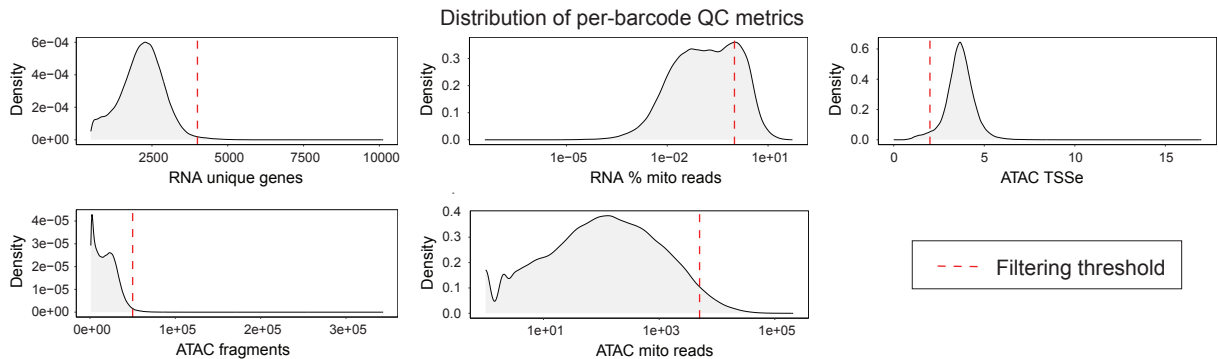
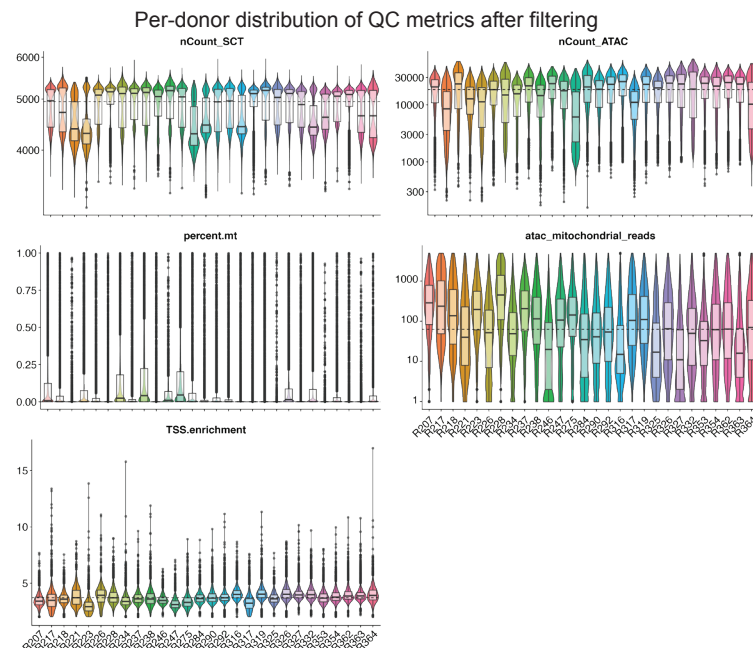
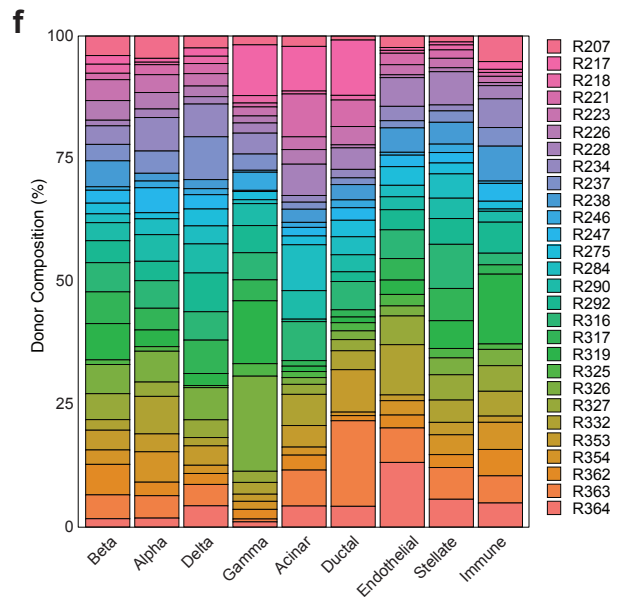
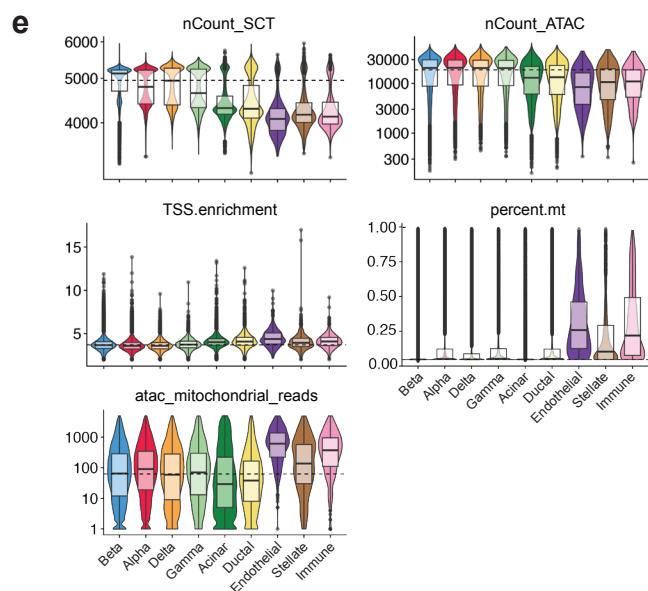
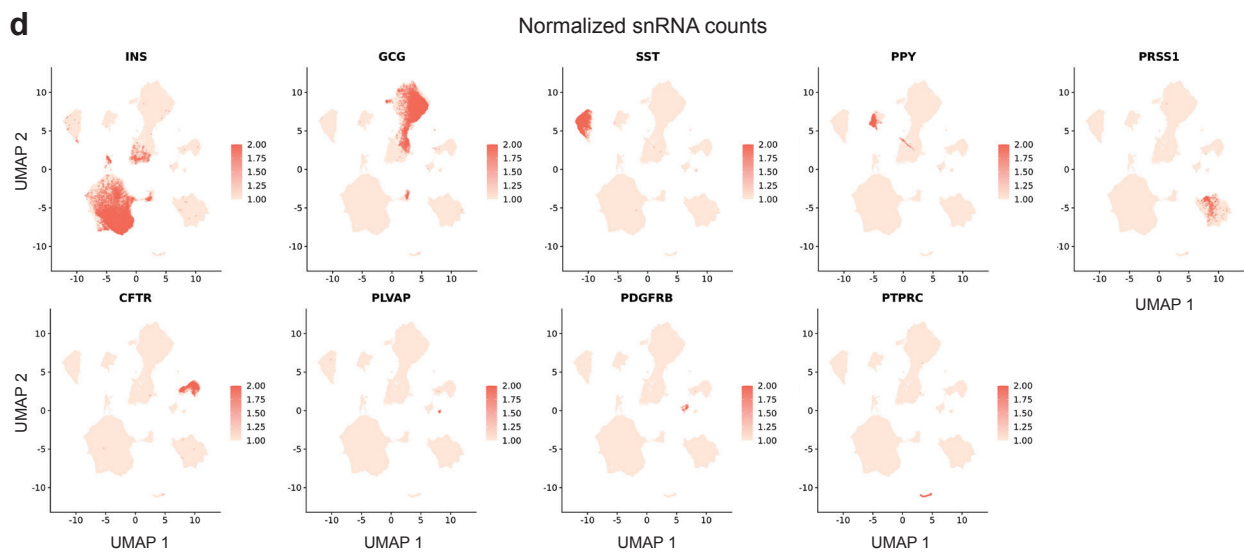
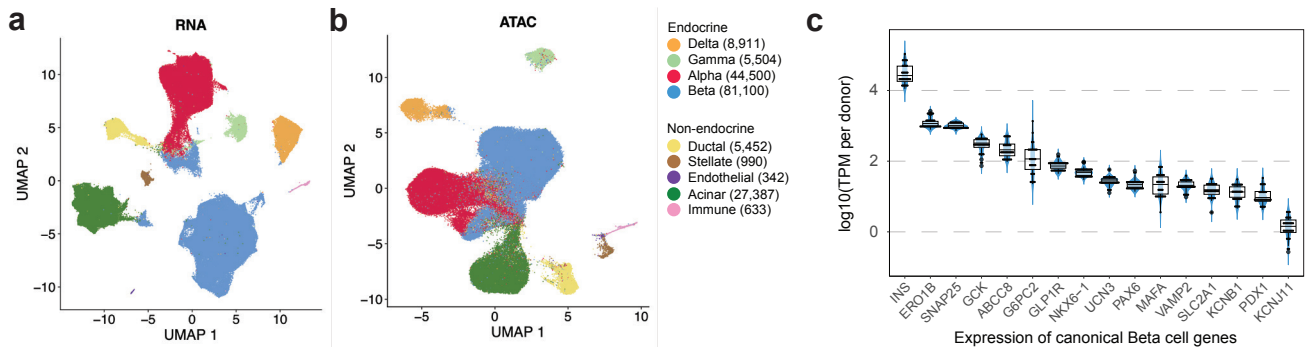


a**b****c****d**

Donor	Amulet doublets	Scrublet doublets	All doublets	Final # cells	Proportion beta cells	SoupX contamination
R207	679	347	867	6248	0.52	0.088
R217	1006	667	1489	5619	0.25	0.038
R218	507	164	619	2172	0.69	0.1474
R221	367	237	515	4902	0.22	0.0265
R223	706	572	1150	6343	0.54	0.0867
R226	416	371	621	5869	0.55	0.0733
R228	772	385	1014	4041	0.23	0.0512
R234	394	509	713	7458	0.41	0.0483
R237	413	343	586	6211	0.44	0.0315
R238	496	317	720	6186	0.69	0.1363
R246	165	97	210	1878	0.30	0.0222
R247	561	336	743	5341	0.40	0.037
R275	940	142	1045	3430	0.51	0.1947
R284	503	486	792	6082	0.24	0.0237
R290	564	636	922	8009	0.37	0.0422
R292	510	343	709	6749	0.54	0.0697
R316	963	928	1464	10752	0.45	0.0357
R317	495	385	780	8531	0.61	0.1325
R319	709	481	972	8942	0.67	0.083
R325	149	107	203	1823	0.42	0.0481
R326	808	869	1247	9798	0.49	0.0308
R327	509	321	686	6820	0.63	0.0445
R332	1125	615	1477	7488	0.23	0.0344
R353	380	470	646	7025	0.46	0.0598
R354	470	337	649	5945	0.40	0.0349
R362	529	311	667	7529	0.67	0.1106
R363	696	751	1038	9469	0.42	0.0418
R364	644	168	772	4159	0.33	0.0269

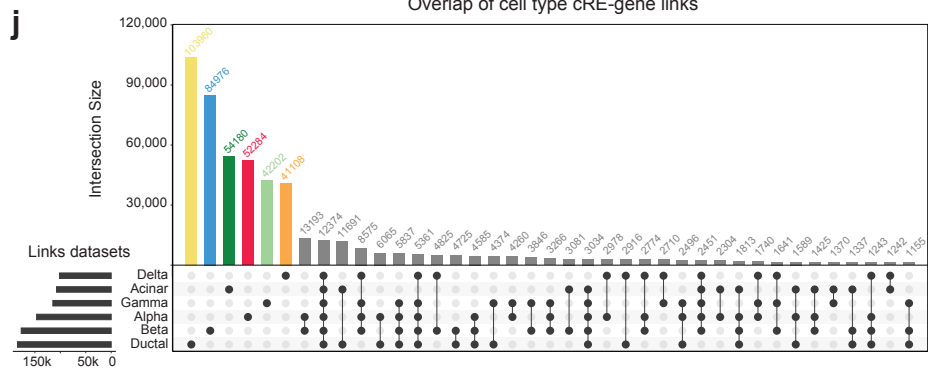
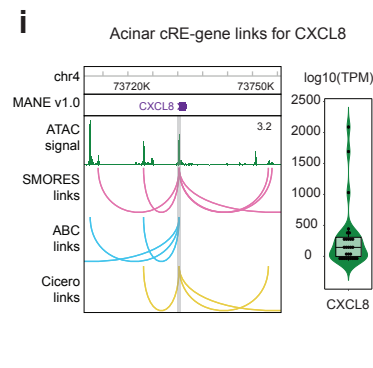
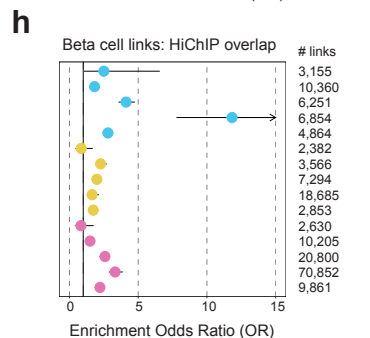
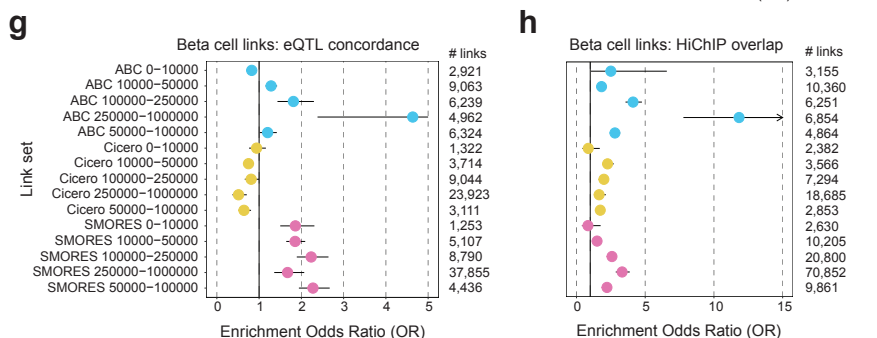
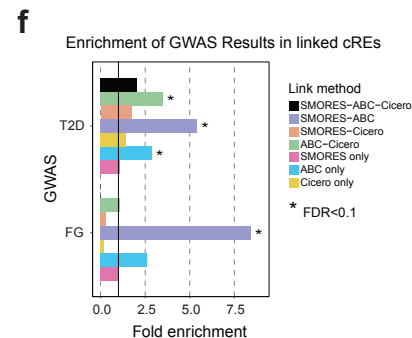
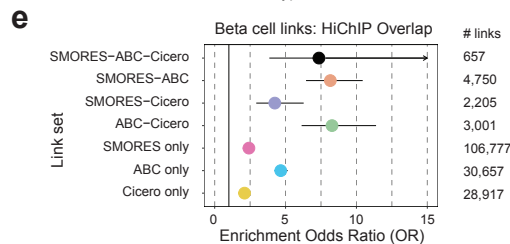
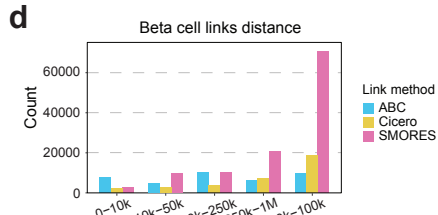
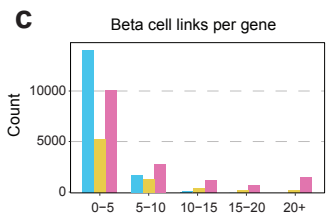
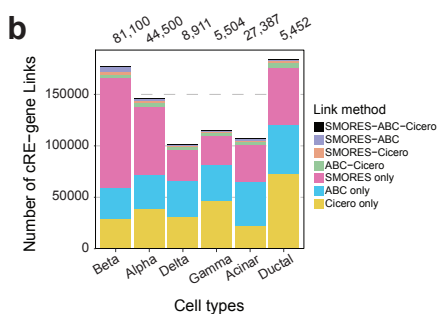
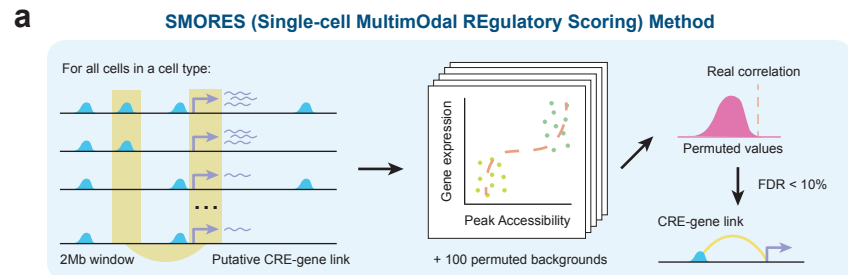
Supplementary Figure 1. Multimodal single cell data processing and quality control

metrics. a) Overview flowchart of our single sample and merged sample processing pipeline for 10x Multiome data. b) Density plots representing the spread of QC metrics in all non-empty droplets, after AMULET doublet removal. The dotted red lines mark the metric cutoffs chosen to remove low quality data barcodes. For RNA unique genes, RNA % mito reads, ATAC fragments and ATAC mito reads these were upper cutoffs; for ATAC TSSe this was a minimum cutoff. c) Violin plots of per-donor distribution of QC metrics after final QC filters were applied. d) Donor level summary of doublets removed, number of barcodes included in the final map, proportion of beta cells and SoupX estimated contamination fraction.

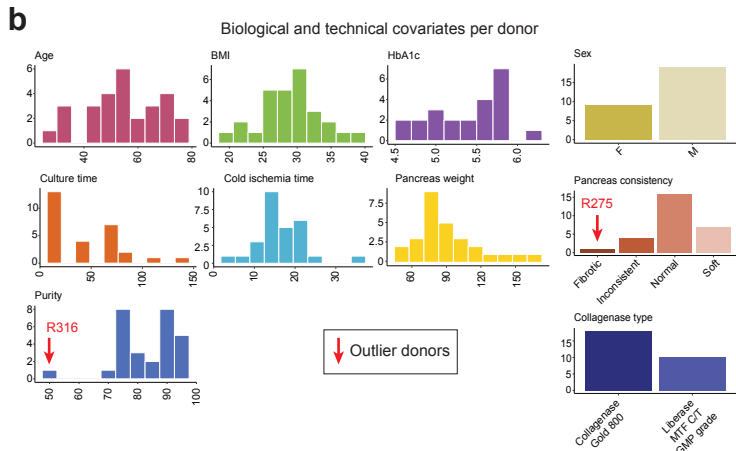
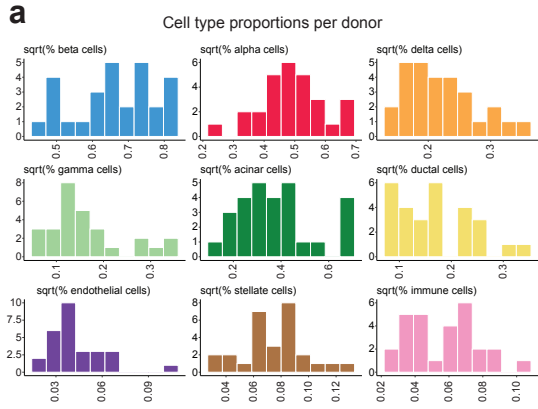


Supplementary Figure 2. Single modality clustering and characterizations of cell type assignments. a-b) Single modality UMAPs of single nuclear RNA (a) and ATAC (b) based clustering of all final barcodes. c) Range of per-donor 'pseudo'-bulk beta cell TPM values for an extended list of canonical beta cell markers. d) SCT-normalized expression of cell type marker genes projected onto the combined modality UMAP. e) Per-cell type distribution of QC metrics after final QC filters were applied. f) Percentage of barcodes from each donor for all cell types.

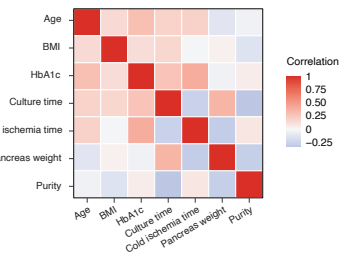
SMORES (Single-cell Multimodal REGULATORY Scoring) Method



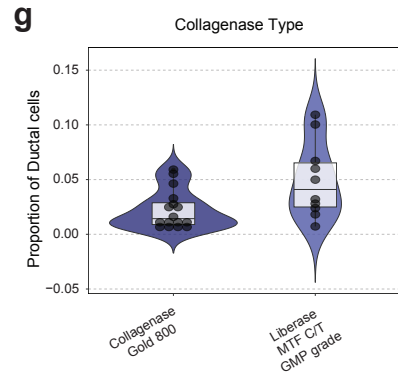
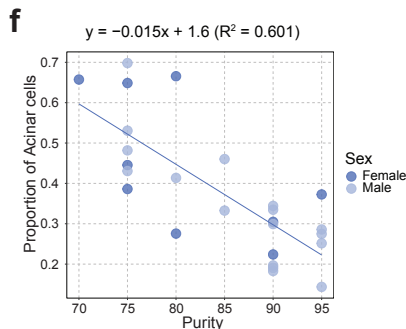
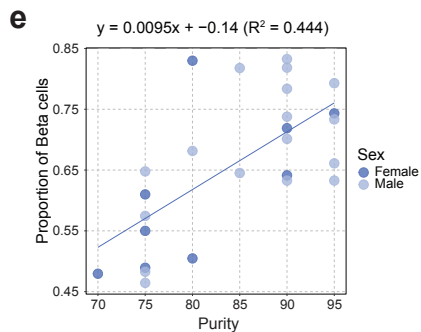
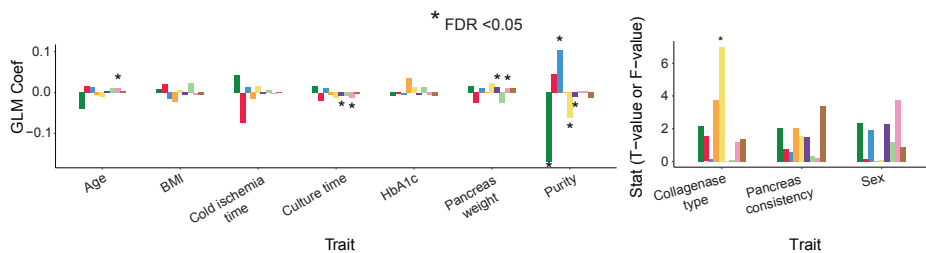
Supplementary Figure 3. Evaluation of prediction methods for cRE-gene target links. a) Overview of Single-cell Multimodal Regulatory Scoring Method (SMORES), for each cREs within a 2Mb window centered around the gene of interest the correlation between binarized cRE accessibility and the gene is calculated and then compared to the correlation generated by 100 permuted barcode sets to generate an empirical p-value. b) Summary of the number of cRE-gene links predicted by each method, or a combination of methods, for each cell type with more than 1,000 barcodes. c-d) Distribution of beta cell cRE-gene links predicted by each method based on number of links per gene (c) and the distance between the cRE and gene TSS (d). e) Acinar cell cRE-gene links between CXCL8 and all cREs predicted to regulate it, separated by prediction method. Right inlay shows the range of per-donor 'pseudo'-bulk acinar cell TPM values for CXCL8. f) Enrichment of eQTLs with the same target gene prediction in cREs of sets of links separated by method and distance between cRE and gene TSS. g-h) Enrichment of overlapping HiChIP genomic contacts in sets of links separated by method and distance (g) and separated by prediction methods (h). i) Enrichment of GWAS credible sets link sets of cRE-gene links separated by prediction methods, as calculated by FINRICH. Stars indicate enrichments passing $FDR < .1$. j) Overlap of all cell type cRE-gene links sets between cell types, for each cell type we are comparing all links generated by any method. The upset plot shows the 40 different cell type overlap combinations with the most links.



c Correlation between continuous covariates



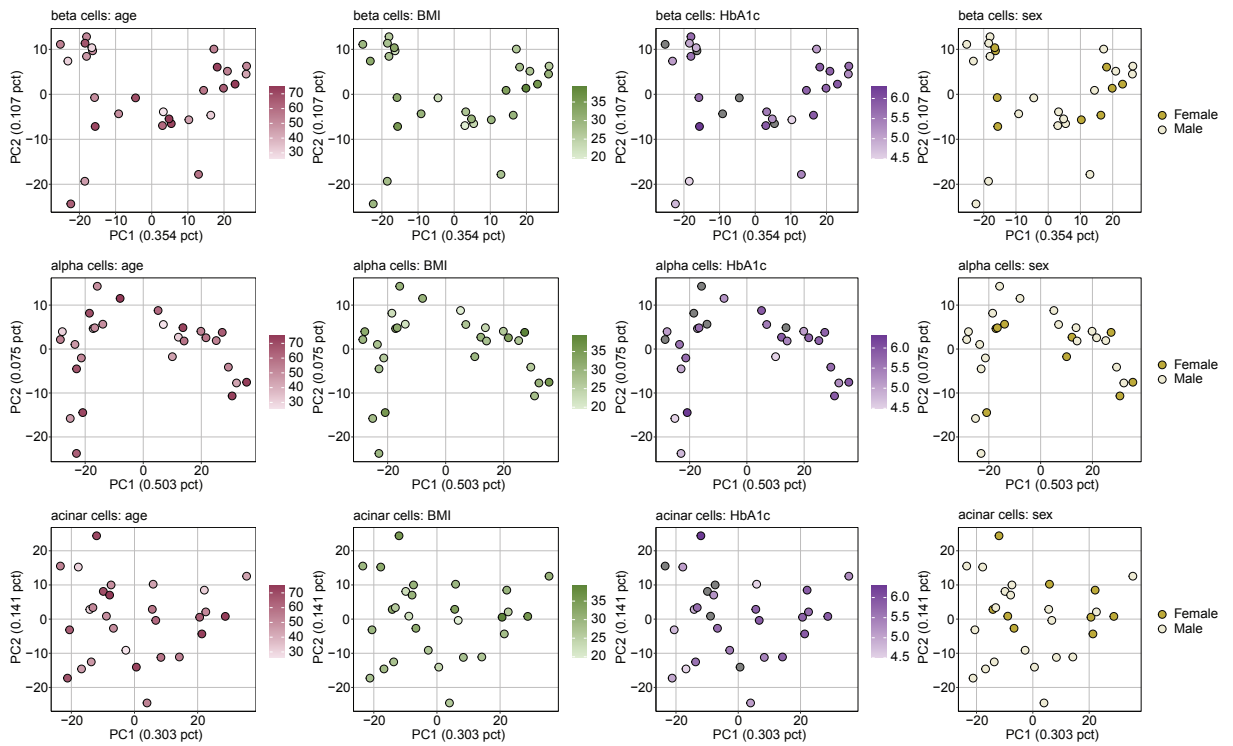
d All cell type proportion vs. trait association results



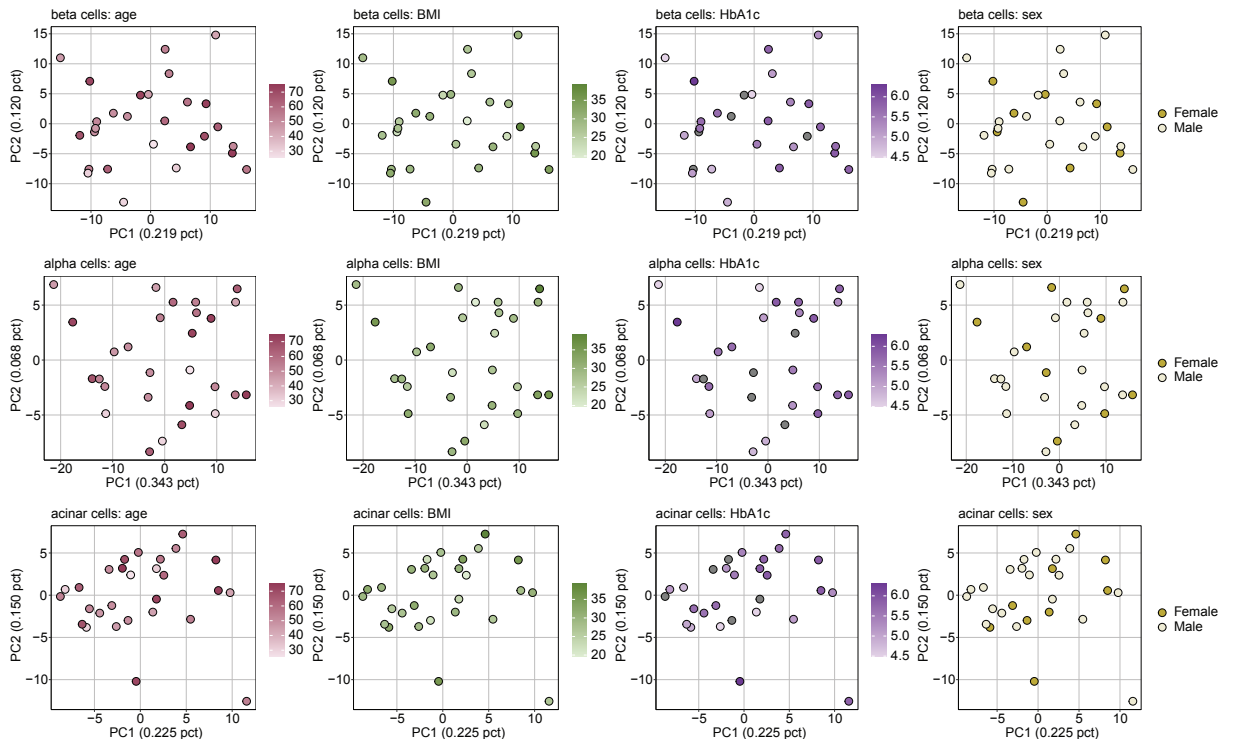
Supplementary Figure 4. Comparisons between cell type proportions and donor covariates. a) Distribution of the proportion of each cell type across donors. Proportion values were scaled by taking the square root of the raw proportion. b) Distribution of biological and technical covariates across all Alberta donors, outlier donors that were not included in proportion associations are indicated with a red arrow. c) Heatmap of the correlation between all continuous covariates. d) Summary of all cell type proportion versus biological and technical covariates associations. For associations with continuous covariates, the coefficient of effect from the linear model is plotted, and for associations with discrete covariates the F value from the ANOVA test is plotted. Significant associates (FDR<.05) are marked with *. e-f) The proportion of beta (e) and acinar (f) cells compared to islet isolation purity. Donor points are colored based on sex: female (dark blue), male (light blue) and a basic linear equation was fit to the relationship, with the equation displayed on top of the graph. g) Distribution of the proportion of ductal cells amongst samples treated with two different collagenase types.

a

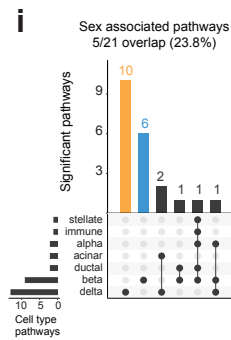
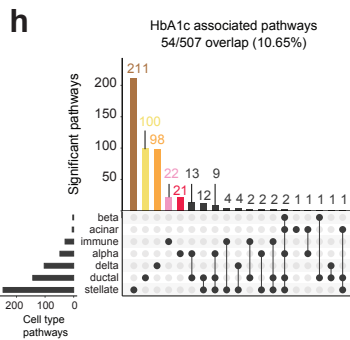
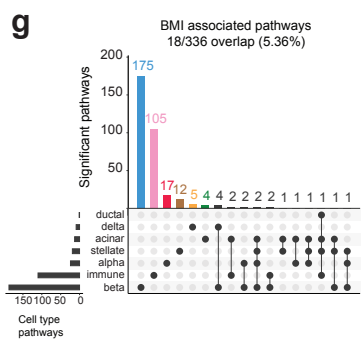
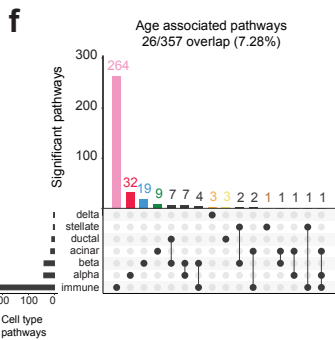
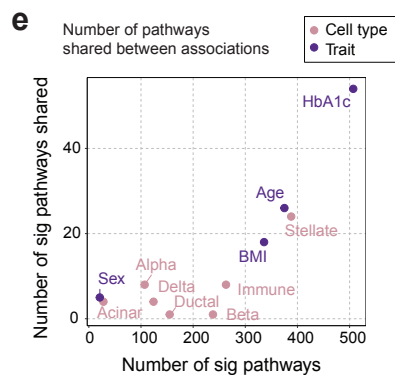
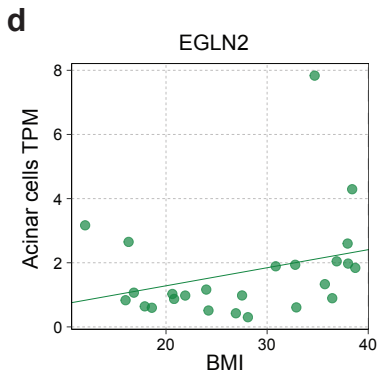
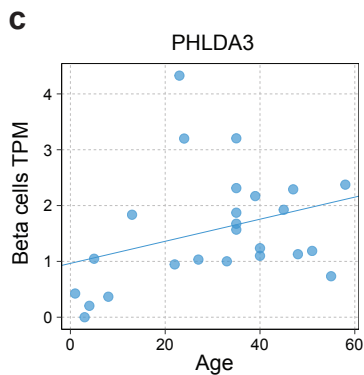
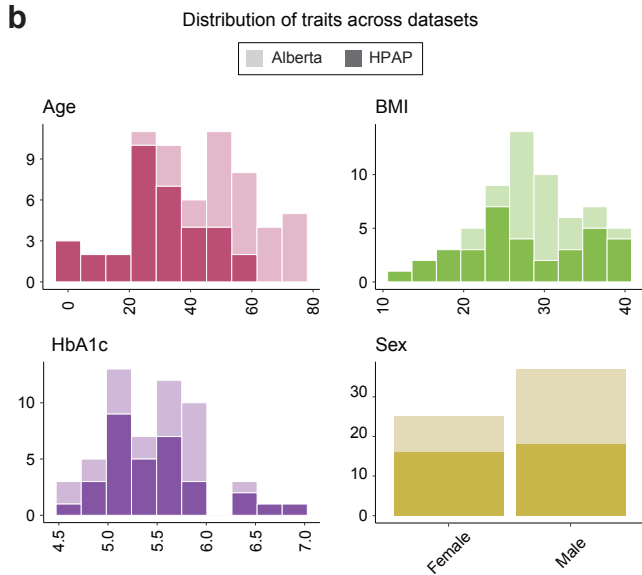
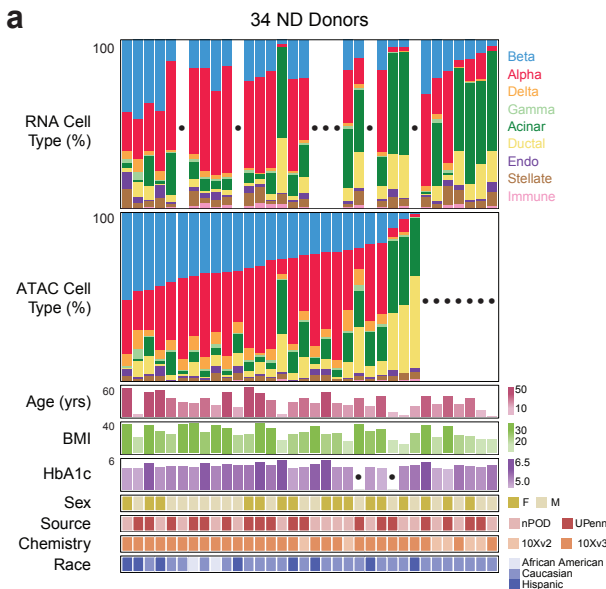
PCA using RNA TPM values

**b**

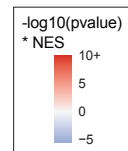
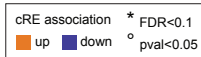
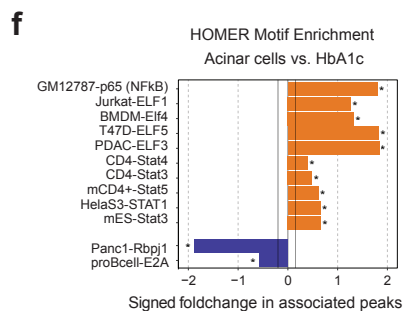
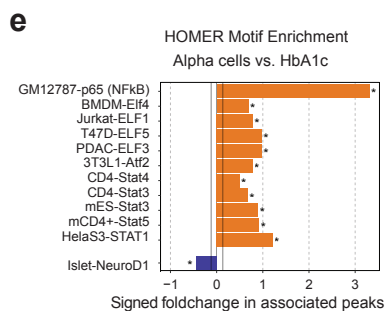
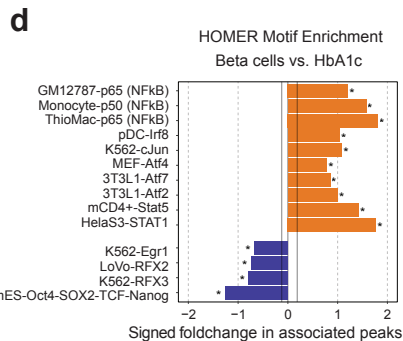
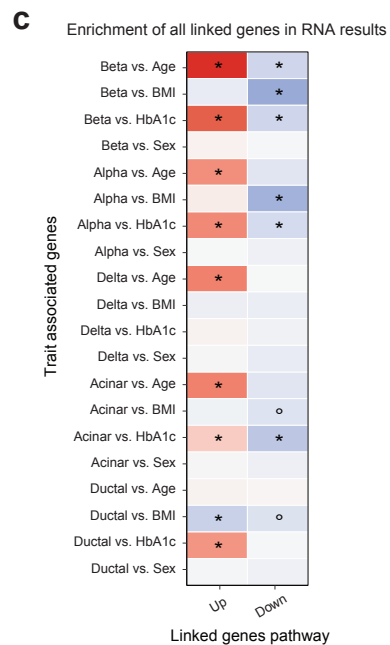
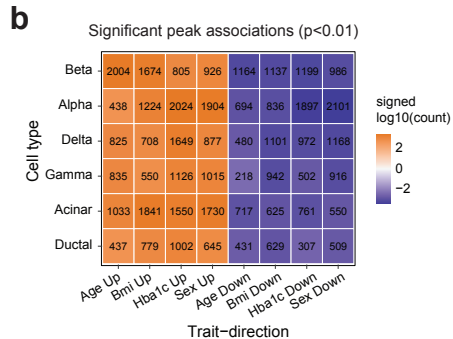
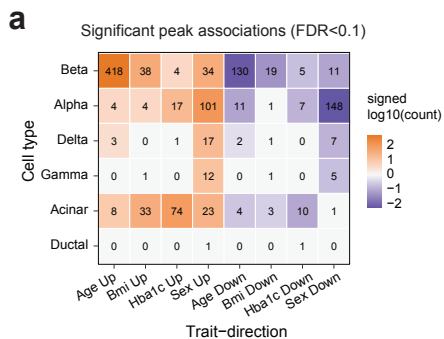
PCA using ATAC CPM values



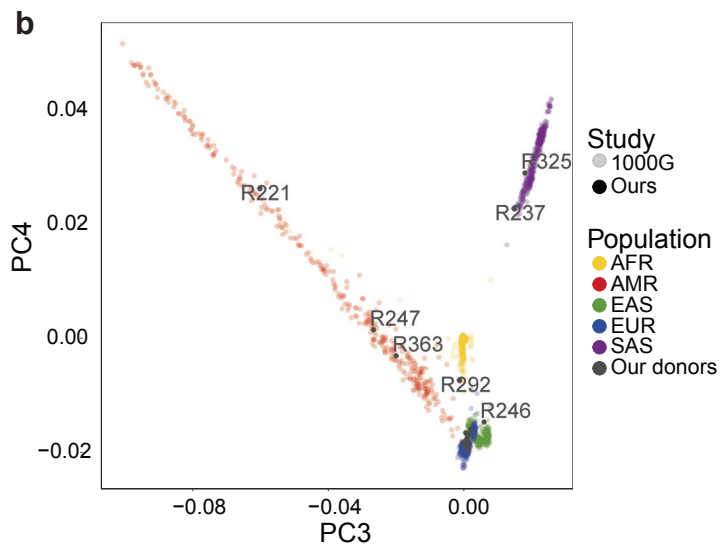
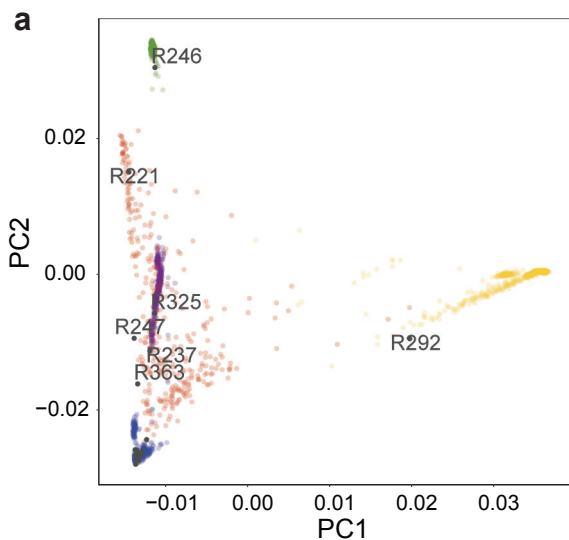
Supplementary Figure 5. Principal component analysis of donor gene expression and chromatin accessibility. a) Donors plotted based on the first and second principal components after performing PCA on per-donor beta, alpha and acinar cell gene expression TPM values. The plots in each column are colored by a different phenotype. b) Donors plotted based on the first and second principal components after performing PCA on per-donor beta, alpha and acinar cell chromatin accessibility CPM values. The plots in each column are colored by a different phenotype.



Supplementary Figure 6. Summary of phenotypes in the HPAP dataset and gene expression associations. a) Distribution of cell type proportions and phenotype information across all 34 non-diabetic HPAP donors, where each column represents a donor. The dots indicate donors with missing measurements, where 17 of the donors had both RNA and ATAC measurements. b) Distribution of phenotypes in donors compared between the two datasets, Alberta (light colors) and HPAP (dark colors). c-d) 'Pseudo'-bulk per-donor TPM values for PHLDA3 (c) and EGLN2 (d) for donors from the HPAP dataset, plotted against age (c) and BMI (d). e) Summary of the overlap in all pathways associated with a trait or a cell type. The numbers of pathways refer to the total number of unique pathways associated with a trait across cell types, or a cell type across traits. Points are labeled based on whether the comparison is of all pathways per a trait (purple), or per a cell type (pink). f-i) Upset plots illustrating the overlap of different pathways associated between cell types and age (f), BMI (g), HbA1c (h) and sex (i).

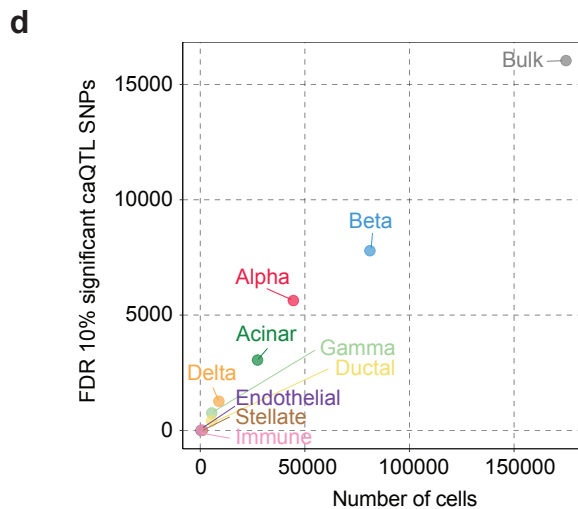


Supplementary Figure 7. Changes in chromatin accessibility associated with donor phenotypes. a-b) Summary of the number of significantly differentially accessible (a; FDR <.1) and nominally differentially accessible (b; p<.01) cREs in associations between cell types and traits. Groups of cREs were divided based on the direction of differential accessibility and then the total number of differential cREs per association was scaled with log₁₀ and signed based on the direction of change. c) Enrichment of all target genes of cREs nominally associated with a phenotype for a cell type in differentially expressed genes associated with the corresponding phenotype. Enrichments were performed by using fGSEA with a database of pathways comprised of all genes linked to a phenotype-associated cRE, split by direction of association. The color of each block is based on the product of the -log₁₀ p-value and the normalized enrichment score (NES) from fGSEA. Nominal (p<.05, °) and FDR significant (FDR<.1,*) enrichments are marked. d-f) HOMER motif enrichment results for cREs increasing (orange) or decreasing (purple) with HbA1c in beta (d), alpha (e) or acinar (f) cells. The solid lines denote the foldchange value associated with the top 20% of motifs tested. Nominal (p<.05, °) and FDR significant (FDR<.1,*) enrichments are marked.

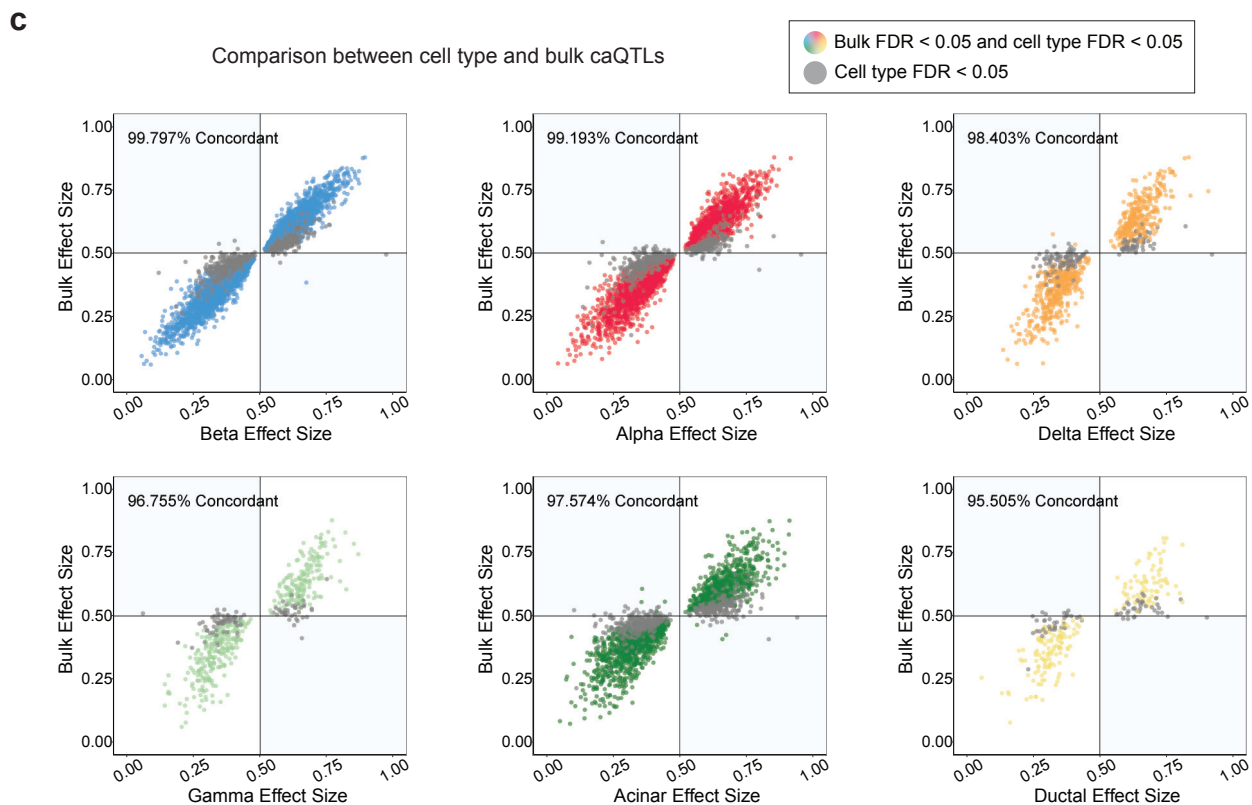
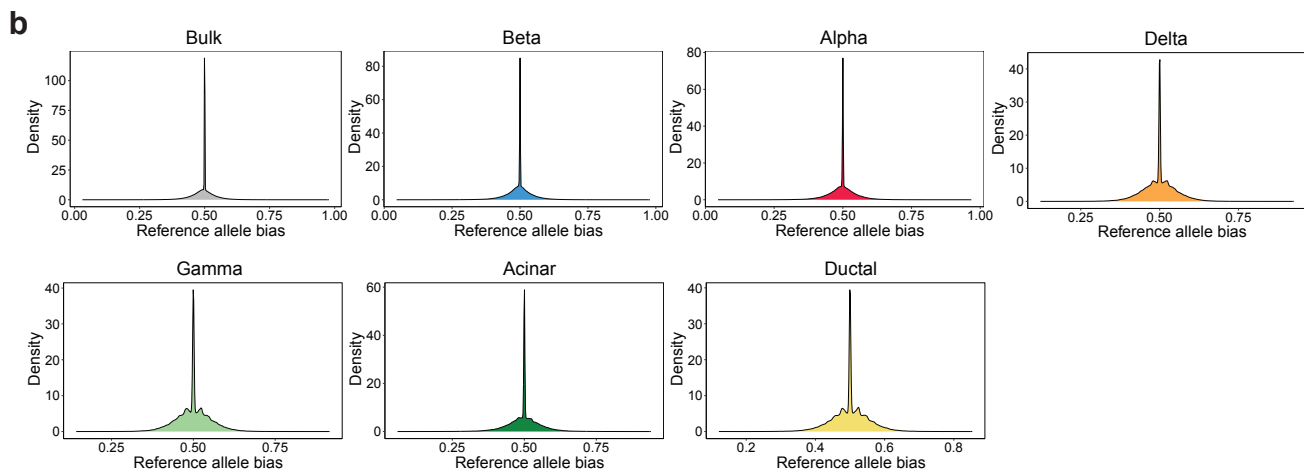
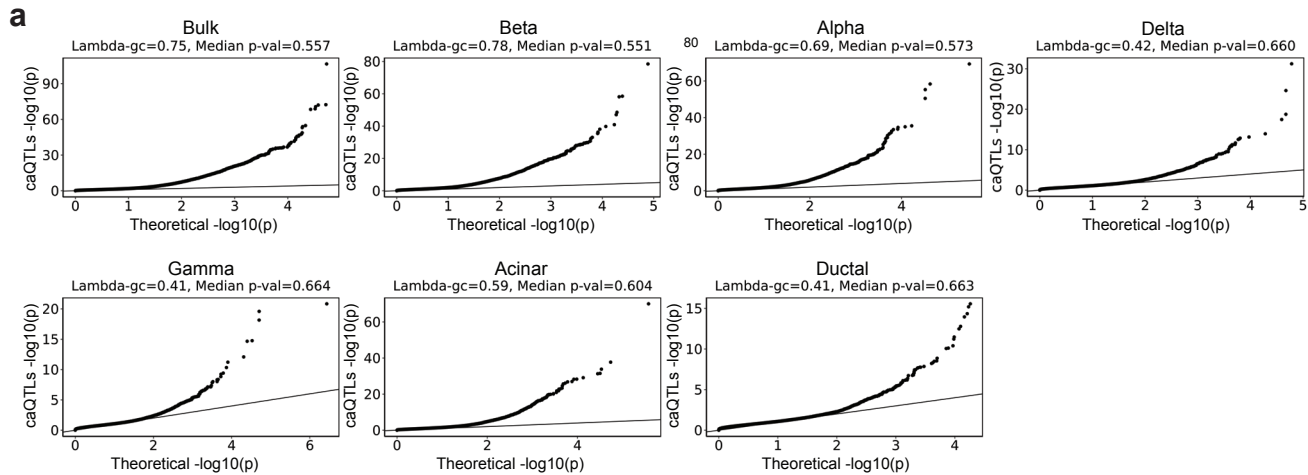


c Summary of caQTL results

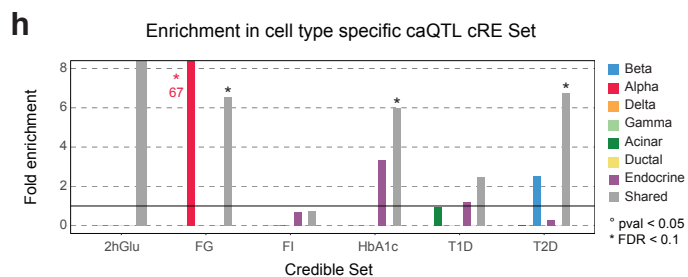
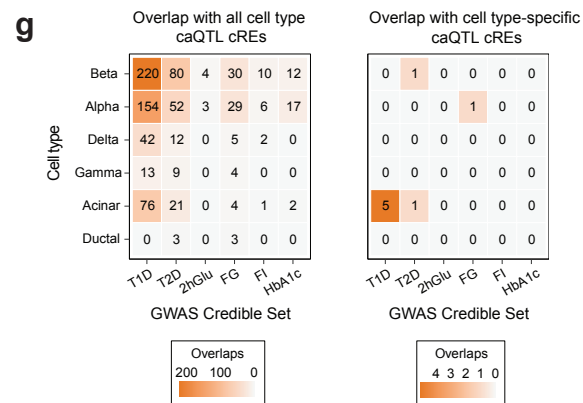
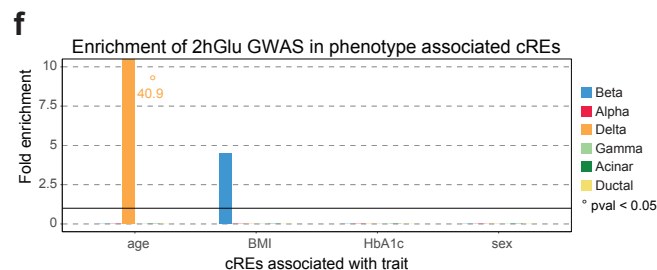
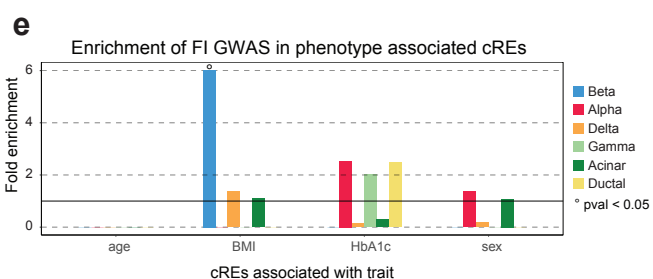
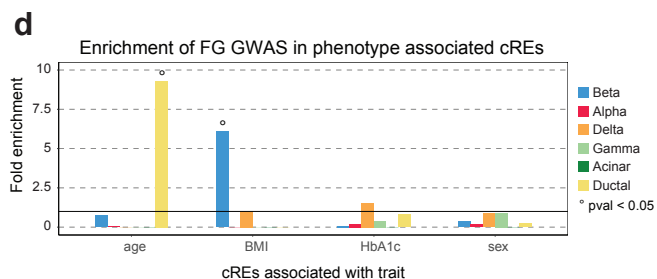
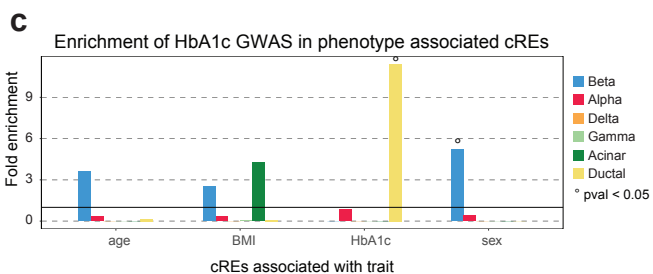
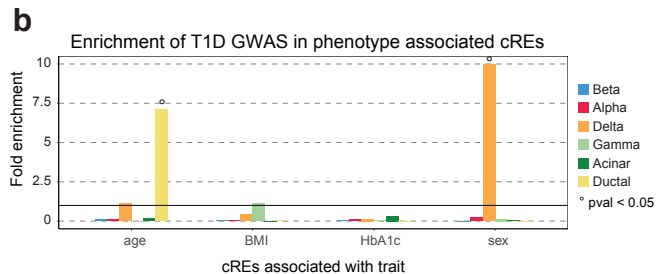
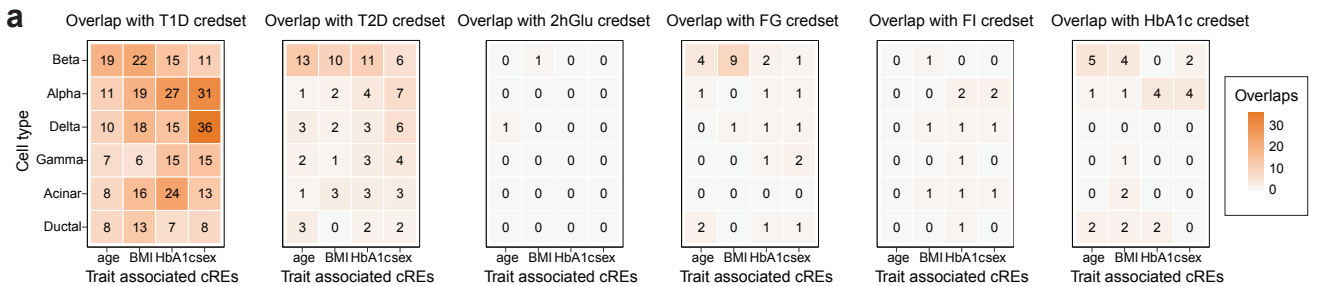
Cell type	caQTL FDR 10%	caQTL FDR 5%	caQTL FDR 1%	Tested features
Bulk	16034	12217	7455	252057
Beta	7789	5932	3657	106506
Alpha	5629	4218	2546	107935
Delta	1262	877	478	79636
Gamma	758	524	274	60138
Acinar	3050	2144	1011	96373
Ductal	419	267	106	49135
Endothelial	0	0	0	1399
Stellate	2	2	2	11915
Immune	9	4	4	8173



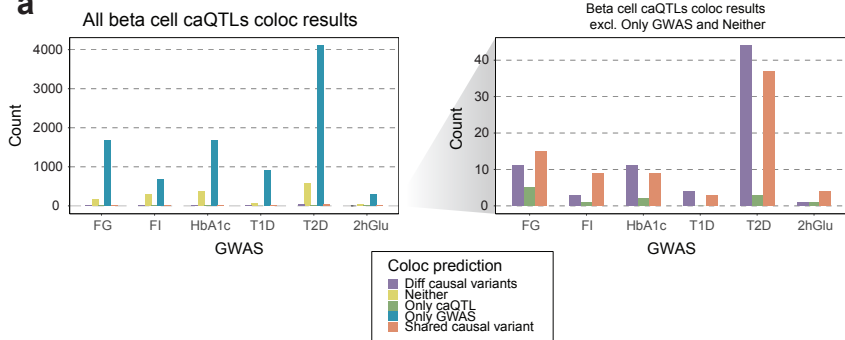
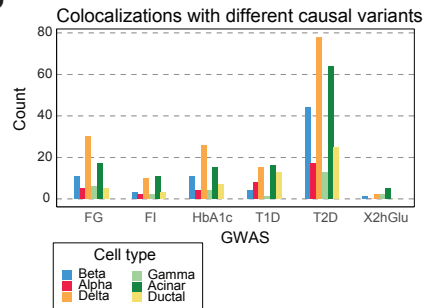
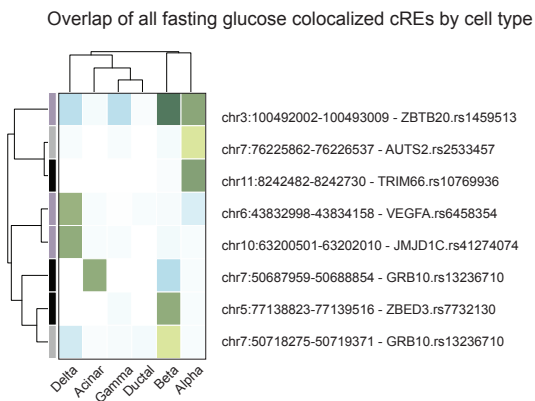
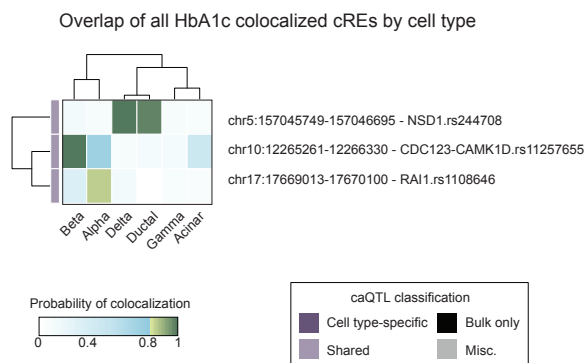
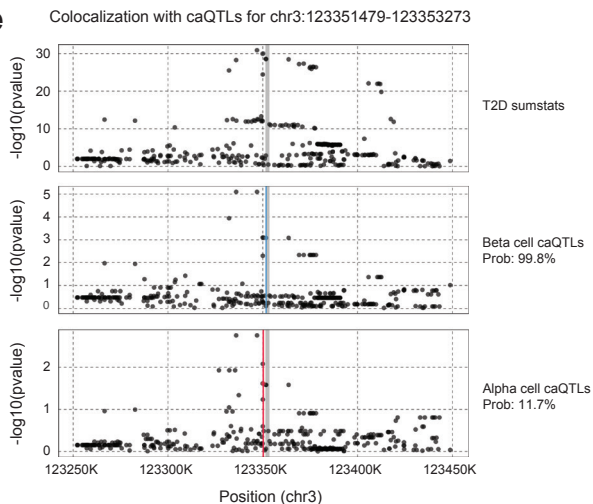
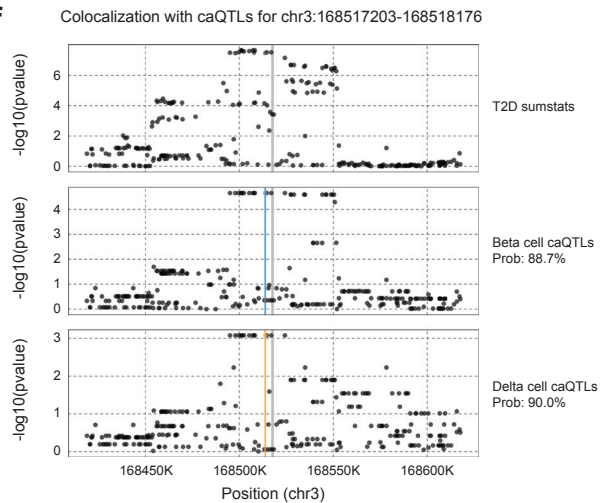
Supplementary Figure 8. Donor ancestries and summary of caQTL results. a-b) Genotype PCA plots for PCs 1 and 2 (a) and PCs 3 and 4 (b). Reference genotypes from the 1000 Genomes project¹⁰² are included and colored according to ancestry group. All donors from our study are colored grey and all non-European donors are labeled with donor ID. c) Summary of caQTLs passing different FDR thresholds, and how many features were initially tested per cell type. d) Comparison between the number of cells in the cell type and the number of significant caQTL SNPs ($FDR < .05$) found in the cell type.



Supplementary Figure 9. caQTL quality control metrics and comparison of cell type caQTLs to bulk. a) Per cell type qq-plots for all caQTL p-values compared to a theoretical uniform distribution. The inflation factor, lambda-GC, and the median p-value for each cell type are listed above each plot. b) Density plots of the distribution of reference allele bias in the caQTLs for all cell types. c) Comparison of caQTL effect size (x-axis) and 'pseudo'-bulk islet caQTL effect sizes (y-axis). All SNPs that are significant cell type caQTLs are included and are colored based on whether they pass FDR significance in the 'pseudo'-bulk. The percentage of variants with concordant directional effects is listed at the top of each plot.



Supplementary Figure 10. Overlap of GWAS credible sets and cREs associated with phenotypes and genotypes. a) Summary of the number of cREs associated with traits that overlap the T1D, T2D, and glycemic trait credible sets. b-f) Enrichment of SNPs in the T1D (b), HbA1c (c), fasting glucose (d), fasting insulin (e), and 2-h glucose after an oral glucose challenge (f) credible sets that overlap cREs associated with age, BMI, HbA1c and sex, in the six largest cell types. Nominally significant enrichments ($p_{val} < .05$) are indicated with °. g) Summary of the number of cREs with one or more significant caQTLs that overlap GWAS credible sets. h) Enrichment of SNPs in the glycemic trait, T1D and T2D credible set that overlap cREs that have a cell type-specific, lineage-specific, or shared significant caQTL in each cell type. FDR significant enrichments ($FDR < .1$) are indicated with * and nominally significant enrichments ($p_{val} < .05$) are indicated with °.

a**b****c****d****e****f**

Supplementary Figure 11. Statistical colocalization between caQTLs and GWAS credible sets. a) Summary of all statistical colocalization results between beta cell caQTLs and all credible sets. For each beta cell cRE, the colocalization prediction with the highest PIP was assigned as the prediction, and what the colored bars represent. Right: zoomed in plot for just colocalizations of different causal variants, only the caQTL has a causal variant, or shared causal variants. b) Summary of the number of statistically significant ($PIP > 0.8$) loci with evidence for different causal variants between cell type caQTLs and summary statistics for glycaemic traits, T1D, and T2D. c-d) The PIP for each fasting glucose (c) and HbA1c (d) colocalized cRE across all cell types. Non-significant colocalizations are colored in blue and significant colocalizations are colored in green. Row names indicate the nearest credible set to the cRE that overlaps GWAS SNPs. e-f) Examples of loci where one or two cell-type caQTLs (e:chr3-123,351,479-123,353,273; f:chr3:168,517,203-168,518,176) colocalized with T2D risk. The lead SNP for each cell type caQTL is indicated by the colored line.

Supplementary Tables and Data

Supplementary Table 1. Characteristics of donors profiled in this study

Supplementary Table 2. Expression level of genes in pancreatic cell types

Supplementary Table 3. Cis-regulatory elements in pancreatic cell types

Supplementary Table 4. Genes with cell type-specific specific expression levels

Supplementary Table 5. Cis-regulatory elements with cell type-specific activity

Supplementary Table 6. Sequence motifs enriched in cell type-specific cREs

Supplementary Table 7. Significant correlations of sample variables with principal components

Supplementary Table 8. Donors from HPAP consortium used in study

Supplementary Table 9. Associations between cell type proportions and donor covariates

Supplementary Table 10. Genes associated with phenotypes in pancreatic cell types

Supplementary Table 11. Gene set enrichment of phenotype-associated genes

Supplementary Table 12. Cis-regulatory elements associated with phenotypes in pancreatic cell types

Supplementary Table 13. Sequence motif accessibility associated with phenotypes in pancreatic cell types

Supplementary Table 14. Sequence motifs enriched in cREs associated with phenotypes

Supplementary Table 15. Sequence motifs enriched in caQTLs for pancreatic cell types

Supplementary Table 16. Enrichment of GWAS signals in sets of phenotype-associated cREs

Supplementary Table 17. Enrichment of GWAS signals in sets of genotype-associated cREs

Supplementary Table 18. Diabetes and glycemic trait loci with pancreatic cell type caQTLs

Supplementary Table 19. Diabetes and glycemic trait loci colocalized with pancreatic cell type caQTLs

Supplementary Data 1. Links between cis-regulatory elements and target genes

Supplementary Data 2. Summary statistics of chromatin QTLs in pancreatic cell types

Supplementary Data 3. Re-estimated chromatin QTL effects in pancreatic cell types